Fixed Switching Frequency Sliding Mode Control for Single-Phase Unipolar Inverters

Adib Abrishamifar, *Member, IEEE*, Ahmad Ale Ahmad, and Mustafa Mohamadian, *Member, IEEE*

***Abstract*—Sliding mode control (SMC) is recognized as robust controller with a high stability in a wide range of operating conditions, although it suffers from chattering problem. In addition, it cannot be directly applied to multiswitches power converters. In this paper, a high performance and fixed switching frequency sliding mode controller is proposed for a single-phase unipolar inverter. The chattering problem of SMC is eliminated by smoothing the control law in a narrow boundary layer, and a pulsewidth modulator produces the fixed frequency switching law for the inverter. The smoothing procedure is based on limitation of pulsewidth modulator. Although the smoothed control law limits the performance of SMC, regulation and dynamic response of the inverter output voltage are in an acceptable superior range. The performance of the proposed controller is verified by both simulation and experiments on a prototype 6-kVA inverter. The experimental results show that the total harmonic distortion of the output voltage is less than 1.1% and 1.7% at maximum linear and nonlinear load, respectively. Furthermore, the output dynamic performance of the inverter strictly conforms the standard IEC62040-3. Moreover, the measured efficiency of the inverter in the worst condition is better than 95.5%.**

***Index Terms*—Pulse width modulator, sliding mode control, uinpolar single phase inverter.**

I. Introduction

NOWADAYS, single-phase pulsewidth modulation (PWM)-based inverter (see Fig. 1), which is used in uninterruptible power supply (UPS), should supply nonlinear and critical step loads. Since the inverter output impedance is not zero, these loads can deform the sinusoidal output voltage of the inverter [1]–[3]. According to the IEEE Standard 1547, the total harmonic distortion (THD) of the output voltage must be less than 5%, especially for nonlinear load. Table I shows the standard details for maximum acceptable harmonic voltage distortion. For inverters with 50-Hz output voltage frequency and its switching frequency higher than 2 kHz, low-frequency harmonics (2nd to 13th) should be rejected by a closed-loop controller perfectly. Moreover, the controller must perform a good regulation of the output voltage against the abrupt variations of the input voltage, output current, and the reference voltage. These demands imply to use a fast controller with good dynamic response for the inverters.

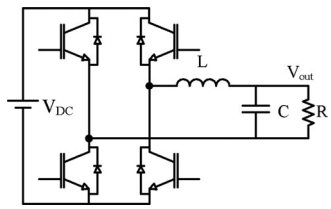

Fig. 1. PWM-based single-phase inverter.

TABLE I
IEEE Standard 1547 for Maximum Acceptable Harmonic Voltage Distortion

Individual Harmonic order	h<11	11≤h<17	17≤h<23	23≤h<35	35≤h	Total Harmonic Distortion
Percent (%)	4.0	2.0	1.5	0.6	0.3	5.0

Recently, many control methods, like repetitive control [4], [5], deadbeat control [6], multiloop feedback [7], [8], hysteresis current mode control [9], and internal model control [10], have been proposed to achieve the aforementioned demands. Occasionally, nonlinear observer [11] and harmonic elimination techniques are employed to improve the transient response. It is noticeable that these control methods are based on average model (small signal model) of the inverter [12], [13], because the inverter state space equations vary when the switches state changes. In this model, discontinuous control quantity, duty ratio of switches, is approximated and modeled by a continuous variable over a number of switching cycles [14]. Thus, it can only well describe the system behavior close to its operating points. In fact, the instantaneous behaviors of the inverter are ignored in the average model and the model is only valid around the operating point.

The inherent switching nature of power converters is compatible with sliding mode control (SMC) feature. The SMC is well known for its robustness, stability, and good regulation properties in a wide range of operating conditions; moreover, it is not necessary to use average model of the inverter [2], [15], [16]. According to the SMC theory, the main subject of the power converter control (with an inherent switching action) is the definition of a good sliding surface and switching condition to guarantee the output voltage regulation with low THD in different conditions [20].

In spite of the SMC excellent performance, it suffers from chattering problem which leads to variable and high frequency

Manuscript received February 8, 2011; revised April 5, 2011, June 9, 2011, July 20, 2011, and September 5, 2011; accepted October 27, 2011. Date of current version February 27, 2012. Recommended for publication by Associate Editor F. L. Luo.

A. Abrishamifar and A. A. Ahmad are with the Department of Electrical Engineering, Iran University of Science and Technology, Tehran 16846-13114, Iran (e-mail: abrishamifar@iust.ac.ir; alahmad_ah@yahoo.com).

M. Mohamadian is with the Department of Electrical and Computer Engineering, Tarbiat Modares University, Tehran 14117-13116, Iran (e-mail: mohamadian@modares.ac.ir).

Color versions of one or more of the figures in this paper are available online at http://ieeexplore.ieee.org.

Digital Object Identifier 10.1109/TPEL.2011.2175249

switching in the converter. This phenomenon increases power losses and also produces severe electromagnetic compatibility (EMC) noise. To fix the switching frequency against line variation for step-down dc/dc converter, Tan *et al*. [17] have introduced an adaptive feedforward control scheme that varied the hysteresis band in the hysteresis modulator of the SM controller in the event of any change of the line input voltage.

Furthermore, authors of [18] have used an adaptive PWM for SMC in which the modulation signal was a constant frequency ramp with variable peak magnitude proportional to the input voltage for a step-down dc/dc converter. The adaptive hysteresis modulator is an effective method to fix the switching frequency, although it suffers from the extra input voltage feedback. It is not also suitable for inverter, because the sliding surface of the inverter is time variant. Authors of [19] only limited the switching frequency of a bipolar inverter from 20 to 40 kHz by computing any time interval and holding the switching action.

In addition to chattering problem, discontinuous control law (switching condition) that is generated by a sign function or hysteresis modulator in the SMC is only suitable for single switch converter such as buck converter due to two stable states of the sign function output [17], [20]. Consequently, the SMC method could not be applied to multiswitch converters such as the single-phase inverters, directly. At least, four stable states are needed to obtain suitable switching pulses for unipolar single phase [21].

In this paper, based on SMC theory, a fixed frequency and high-performance controller is proposed to apply to unipolar single-phase inverters. A pulsewidth modulator is employed to fix the switching frequency and to generate the suitable switching law for the four switch inverter.

II. SMC

One effective control tool compliant with the switching nature of the inverter is represented by SMC, which is derived from the variable structure system theory. This control method has individual advantages for control of converters such as

1) stability against severe variations of load and the line;
2) robustness;
3) good dynamic response;
4) very simple implementation.

Based on SMC theory, a discrete control law can be defined for each system in which the system states X follow desired states X_d. The discrete control law is as follows:

$$u = \operatorname{sign}(S(X)) = \begin{cases} +1 & \text{if } S(X) > 0 \\ -1 & \text{if } S(X) < 0 \end{cases} \tag{1}$$

where $S(X)$ is a scalar function and $S(X) = 0$ is called switching or sliding surface. This function is defined as

$$S(X) = \left(\frac{d}{dt} + \lambda\right)^{n-1} (X - X_d) \tag{2}$$

where n is the system order ($n \neq 1$) and λ is a strictly positive constant. According to Lyapunov theorem, to ensure the stability of the system, the following inequality should be established

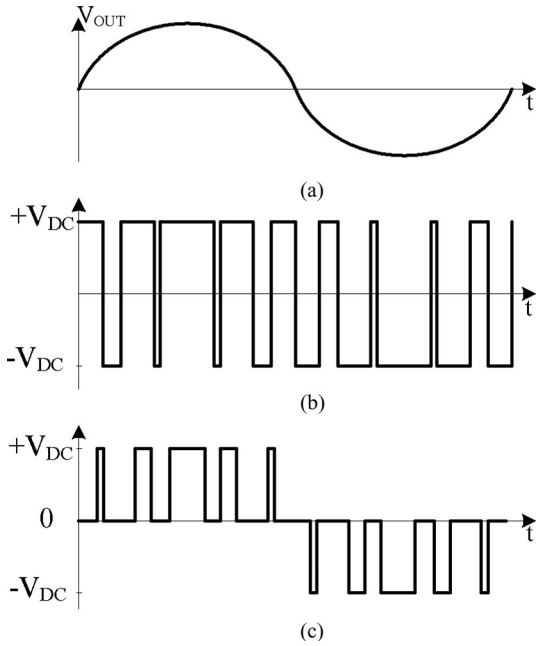

Fig. 2. (a) Inverter output voltage. (b) Bipolar PWM. (c) Unipolar PWM.

while η is a strictly positive constant:

$$\frac{1}{2}\frac{d}{dt}S^2 \leq -\eta\,|S|\,. \tag{3}$$

This means that

$$\begin{cases} \lim\limits_{S\to 0^+} S(X) > 0 \\ \lim\limits_{S\to 0^-} S(X) < 0 \end{cases}, \quad \begin{cases} \lim\limits_{S\to 0^+} \dot{S}(X) < 0 \\ \lim\limits_{S\to 0^-} \dot{S}(X) > 0. \end{cases} \tag{4}$$

If conditions (4) or sliding conditions are established, starting from any initial condition, the discontinuous control law u makes the state trajectory to reach the sliding surface in a finite time, and then slides along the surface toward X_d exponentially. In the sliding mode, the system dynamic response is represented by $S(X) = 0$.

III. Unipolar Single-Phase Inverter

There are two popular PWM techniques (see Fig. 2), applying to single-phase inverters, unipolar and bipolar PWM.

The unipolar PWM employs $+\mathrm{V_{DC}}$ and zero to provide positive outputs, and $-\mathrm{V_{DC}}$ and zero to provide negative outputs, but the bipolar PWM only uses $+\mathrm{V_{DC}}$ and $-\mathrm{V_{DC}}$ to make either positive or negative outputs. Hence, carrier harmonic content in the bipolar scheme is twice of unipolar scheme. Notice that, in the unipolar technique, the output voltage does not contain even harmonics and also the first high-frequency harmonic appears around twice of the switching frequency and not at the switching frequency as it would have been in the case of bipolar PWM. Because of these three attractive features of the unipolar PWM, we develop unipolar PWM in this paper.

The ac output voltage of the inverter can be written as

$$V_{\mathrm{out}} = V_{\mathrm{DC}} \times m \times \mathrm{Sin}(2\pi f_o t) \tag{5}$$

where $V_{\rm out}$, $V_{\rm DC}$, m, and f_o represent the output voltage, the input voltage, modulation factor, and output frequency, respectively. Assuming ideal elements, the state equations of the inverter are

$$\begin{cases} L\dfrac{di_L}{dt} = u \times V_{\rm DC} - V_{\rm out} \quad u = -1, 0, +1 \\ C\dfrac{dV_{\rm out}}{dt} = i_C = i_L - i_{\rm o} \\ i_{\rm o} = \dfrac{V_{\rm out}}{R} \end{cases} \tag{6}$$

where inductor current i_L and output voltage $V_{\rm out}$ are selected as state variables. u is the discontinuous input of the system. It is 0 or 1 to provide positive output and, 0 or -1 to provide negative output. In addition, i_c, i_o, and R are the capacitor current, output current, and load, respectively. To implement the SMC for the inverter, it is more convenient to use a system description, which involves the output error and its derivative

$$\begin{cases} e = V_{\rm out} - V_{\rm ref} \\ \dot{e} = \dfrac{d}{dt}(V_{\rm out} - V_{\rm ref}) = \dfrac{i_C}{\rm C} - \dot{V}_{\rm ref} \end{cases} \tag{7}$$

where $V_{\rm ref}$ is the reference voltage. In the inverter, the output voltage is forced to be equal to $V_{\rm ref}$ by appropriate switching.

Considering continuous current mode operation of the inverter and, selecting the e and $\dot{e}$ as state variables, the system equations in terms of the state variables x_1 and x_2 can be rewritten as follows

$$\begin{cases} x_1 = V_{\rm out} - V_{\rm ref} \\ x_2 = \dot{x}_1 = \dfrac{i_C}{C} - \dot{V}_{\rm ref} \end{cases} \tag{8}$$

and

$$\begin{cases} \dot{x}_1 = x_2 \\ \dot{x}_2 = -\dfrac{x_1}{LC} - \dfrac{x_2}{RC} - \dfrac{V_{\rm in}}{LC}u - \dfrac{V_{\rm ref}}{LC}. \end{cases} \tag{9}$$

Now, we should define an appropriate sliding surface and switching condition for desirable control of the inverter. Based on (2), the sliding surface can be defined as follows:

$$S(X) = \left(\frac{d}{dt} + \lambda\right) x_1 = \dot{x}_1 + \lambda x_1 = x_2 + \lambda x_1 = 0. \tag{10}$$

To establish the sliding condition for the inverter, λ should be selected to satisfying

$$\lambda\left(\lambda - \frac{1}{RC}\right) > -\frac{1}{LC}. \tag{11}$$

As mentioned before, direct implementation of switching control law through sign function of $S(X)$ is not capable to apply the inverter. Smooth control law and pulsewidth modulator are employed to overcome it practically.

Generally, the chattering problem is eliminated by smoothing the control discontinuity in a narrow boundary neighboring the sliding surface [22]. Accordingly, in the boundary layer, discontinuous control law, $u(u = -\text{sign}(S(X)))$, is replaced by $S(X)/\Phi$ (see Fig. 3). The smoothed control law increases the tracking error and also, decreases the robustness to unmodeled dynamics. Therefore, selection of Φ is a tradeoff between tracking error and the smoothing of control discontinuity.

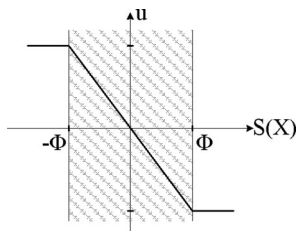

Fig. 3. Smoothed control law in the boundary layer.

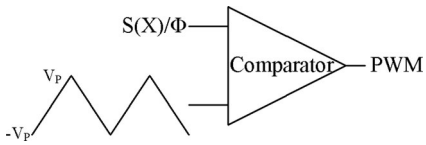

Fig. 4. Pulsewidth modulator.

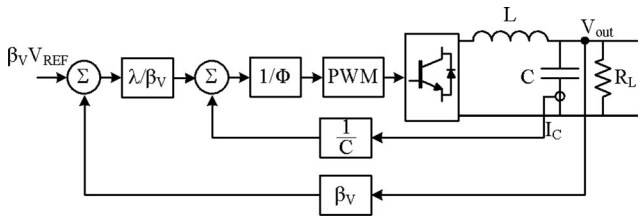

Fig. 5. Proposed controller for single-phase inverters.

Now, to provide switching law for the inverter, we apply the smooth control law to a pulsewidth modulator (see Fig. 4). It also results the inverter with a fixed switching frequency.

Our control loop is illustrated in Fig. 5 which is proposed from the previous description about the control system. It consists of two control loops, outer voltage loop and inner capacitor current loop, with a pulsewidth modulator.

In the pulsewidth modulator, the slope of triangle carrier must be higher than the slope of the input signal. The slope of triangle carrier S_C is

$$S_C = 4V_P \times f_{\rm S} \tag{12}$$

where V_P and f_s are the triangle carrier amplitude and frequency, respectively.

In the proposed control method, the input of pulsewidth modulator, $S(X)/\Phi$, consist of two terms: error of the output voltage and the error of the capacitor current

$$\begin{aligned} \frac{S(X)}{\Phi} &= \frac{x_2 + \lambda x_1}{\Phi} = \frac{i_C}{C\Phi} - \frac{\dot{\rm V}_{\rm ref}}{\Phi} + \frac{\lambda}{\Phi}(V_{\rm out} - V_{\rm ref}) \\ &= \frac{1}{\rm C\Phi}(i_C - i_{\rm ref}) + \frac{\lambda}{\Phi}(V_{\rm out} - V_{\rm ref}). \end{aligned} \tag{13}$$

In the steady state, the inverter output voltage can be assumed a pure sinusoidal waveform and its error is very close to zero. Since the inductor ripple current ΔI_L is entered to the capacitor, the capacitor current error is equal to the inductor ripple current,

TABLE II
SIMULATED INVERTER CHARACTERISTICS

V_{DC}	350V
V_{out}	$220V_{RMS}$
S_{out}	6KVA
f_s	15KHz
F	50Hz
L	357μH
C	9.4μF
R (full load)	27.5Ω
f_r	2750Hz

and (13) can be reduced to

$$\frac{S(X)}{\Phi} \approx \frac{1}{C\Phi}(i_C - i_{\rm ref}) = \frac{\Delta I_L}{C\Phi}. \tag{14}$$

Since the capacitor ripple current is very steep, the input signal of the pulsewidth modulator may be very high slope. So, proper selection of Φ can aim to reduce the rapid slope of the PWM input signal. According to [21]

$$\Delta I_L = \frac{V_{\rm DC} - V_{\rm out}}{L} DT \tag{15}$$

and

$$D = m \times \mathrm{Sin}(2\pi f_o t) \tag{16}$$

where D and T are time-dependent duty ratio and period of triangle carrier, respectively. Substituting (5), (15), and (16) into (14), then derivation on T, the slope of the input signal $S_{\rm IN}$ yields

$$S_{\rm IN} = \frac{V_{\rm DC}}{4LC\Phi}. \tag{17}$$

Now, according to the limitation on the pulsewidth modulator, the minimum of Φ is obtained as follows:

$$\frac{V_{\rm DC}}{4LC\Phi} \ll 4V_P \times f_S. \tag{18}$$

Then

$$\frac{V_{\rm DC}}{16LCV_P f_S} \ll \Phi \Rightarrow \frac{10V_{\rm DC}}{16LCV_P f_S} \approx \Phi_{\min}. \tag{19}$$

IV. SIMULATION RESULTS

The proposed control method has been simulated by Simulink Toolbox in MATLAB for an inverter whose main characteristics are mentioned in Table II, in which f_s and f_r are switching frequency and cutoff frequency, correspondingly.

Controller parameters of the simulated inverter are listed in Table III. β_V is selected considering the electronic circuit's limitation. In accordance with (10), the inverter dynamic response is of first order with time constant $\tau = 1/\lambda$. Moreover, the response time of inverter cannot be faster than a period of switching; therefore, we chose $\lambda_{\max} = f_s$.

The THD of output voltage is about 0.78% and 1.6% at maximum linear and nonlinear load, respectively. Fig. 6 represents

TABLE III
CONTROLLER PARAMETERS

β_V	0.022727
λ	15000
$\Phi_{\min}$	134751
V_P	8(V)

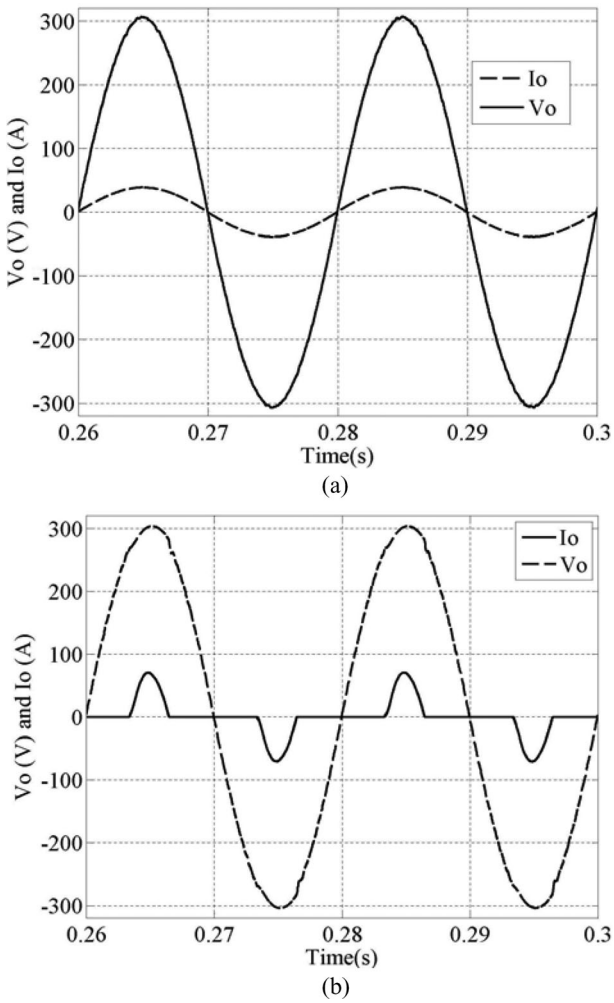

Fig. 6. Simulation result. a) Output voltage and current at 6-kW linear load. b) Output voltage and current at 6-kVA nonlinear load with CF = 2.75 and PF = +0.7.

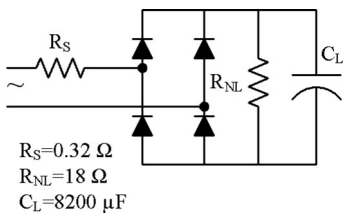

Fig. 7. Nonlinear load according to IEC62040-3 standard.

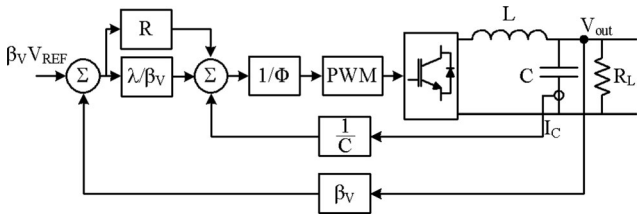

Fig. 8. Proposed controller for single-phase inverters with a resonator in voltage loop.

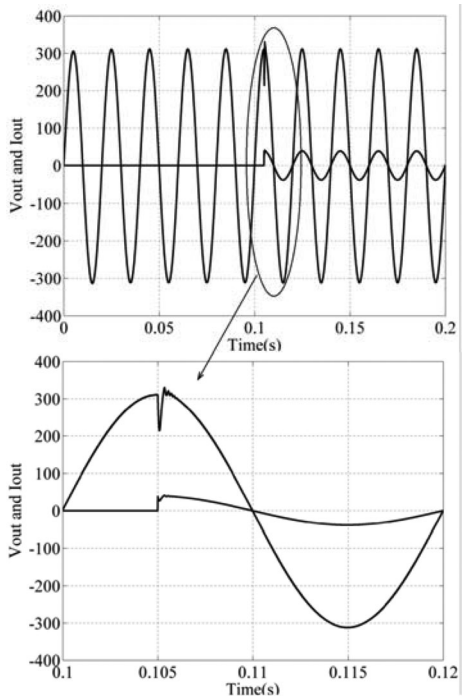

Fig. 9. Simulation result: transient response of the output voltage for linear step load from zero to 100%.

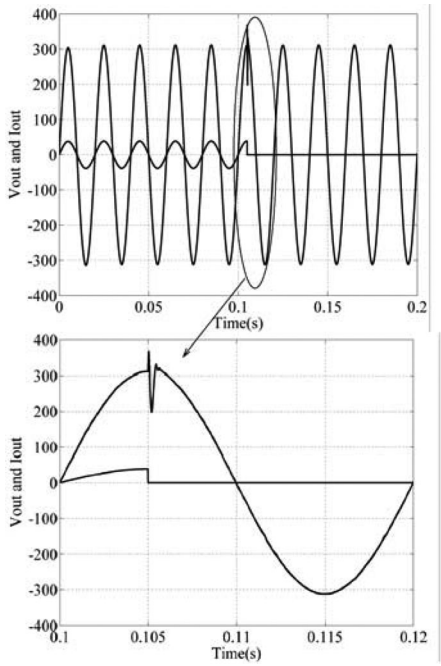

Fig. 10. Simulation result: transient response of the output voltage for linear step load from 100% to zero.

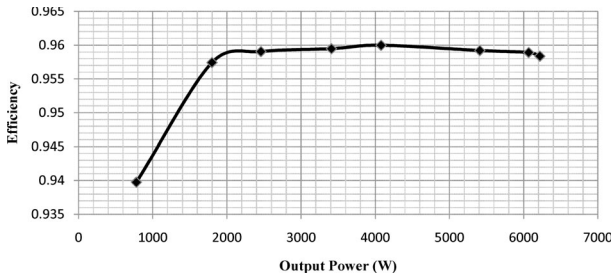

Fig. 11. Experimental result: efficiency of inverter versus output power.

the output voltage and current at maximum linear and nonlinear load. The nonlinear load was designed according to IEC62040-3 standard (see Fig. 7). The crest factor (CF) and the power factor (PF) of the nonlinear load are about 2.75 and +0.7, respectively.

Simulation results also show that the transient time is below 0.3 ms for applying standard step load which means that the dynamic performance of this inverter severely complies with the class 1 UPS of IEC6204-3. The load regulation is also about 1%. That is sufficient for many applications. However, to obtain better regulation for especial applications, a resonance compensator is employed in the voltage loop controller (see Fig. 8). The resonance compensator is described by the practical transfer function as follows [23]:

$$G_R = \frac{k_R s}{s^2 + 2\pi\Delta f\, s + (2\pi f_o)^2} \tag{20}$$

which produces a forward high gain at f_o equal to $G_R = k_R/(2\pi\Delta f)$. k_R and Δf are the compensator coefficient and cutoff frequency, respectively. With this new controller, the regulation is better than 0.2%.

Figs. 9 and 10 present the output voltage and current behavior at step load condition. The output voltage undershoot is less than 26% and also the settling time is about 0.2 ms for the linear step load from zero to 100%. The output voltage overshoot, due to linear step load from 100% to zero, is less than 20% and also the settling time is about 0.3 ms. Furthermore, the load and line regulation are 0.2% and 0.5%, respectively.

V. Experimental Results

The inverter was implemented and tested experimentally. The inverter bridge consists of four 500-V, 50-A power MOSFETs. A 1.2-μS dead time is considered in switching of MOSFETs to prevent shoot through (the accidental short circuit in the inverter leg). The inductor of the output filter is made with EE128 ferrite core, with 2.5-mm air gap. Furthermore, the filter capacitance consists of two parallel 4.7-μF, 400-V ceramic capacitors.

Efficiency of the inverter is measured up to 95.5% (see Fig. 11). The power loss of the inverter is also about 43 W at the no load condition ($R = \infty$). The THD of output voltage is 0.9% and 1.1% at minimum and maximum linear load,

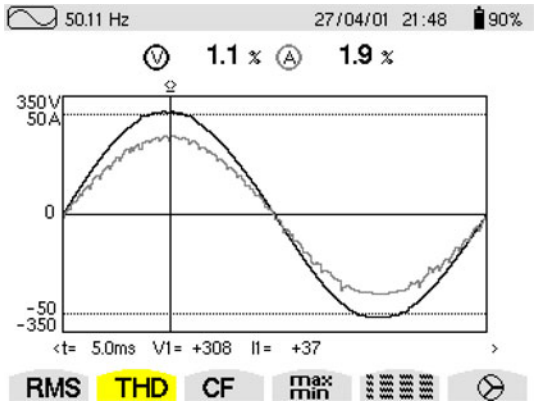

Fig. 12. Experimental result: output voltage and current at maximum linear load (6 kW).

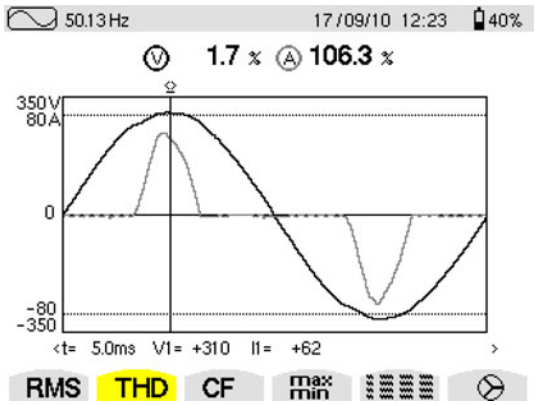

Fig. 13. Experimental result: output voltage and current at maximum linear load, CF = 2.75.

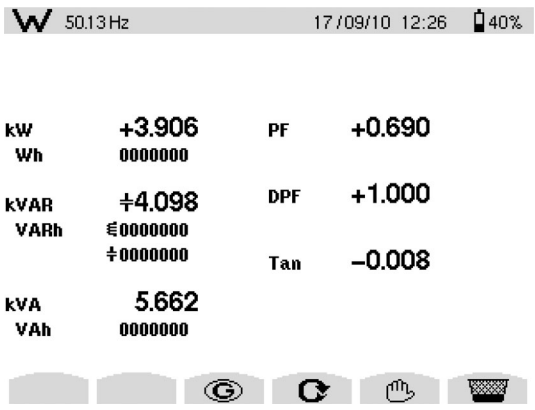

Fig. 14. Experimental result: details of output power at nonlinear test.

correspondingly. Fig. 12 indicates the output voltage and current at maximum linear load (6 kW). The voltage and current were measured by C.A 8334B, Chauvin Arnoux, network analyzer.

Fig. 13 shows the output voltage and current at maximum nonlinear load whose CF is equal to 2.75. It is seen that the THD of output voltage is 1.7%. Details of the nonlinear load are presented in Fig. 14. The apparent power of the nonlinear load is 5.66 kVA whose PF is +0.69.

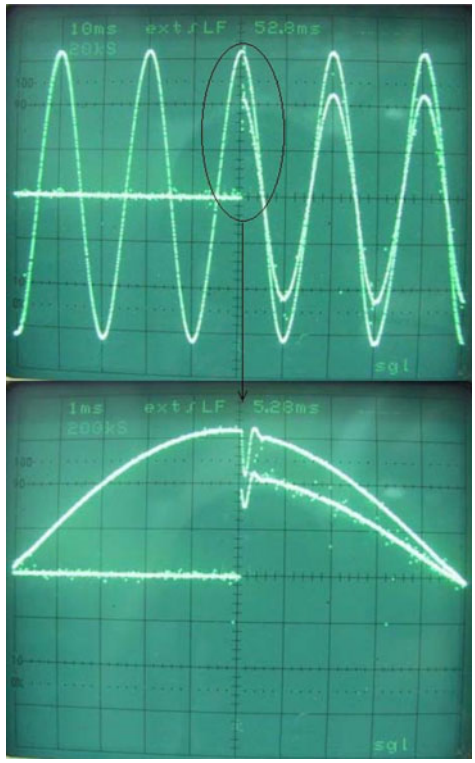

Fig. 15. Experimental result: Transient response of the output voltage for linear step load from zero to 100%, voltage scale = 100 V/div, and current scale = 19 A/div.

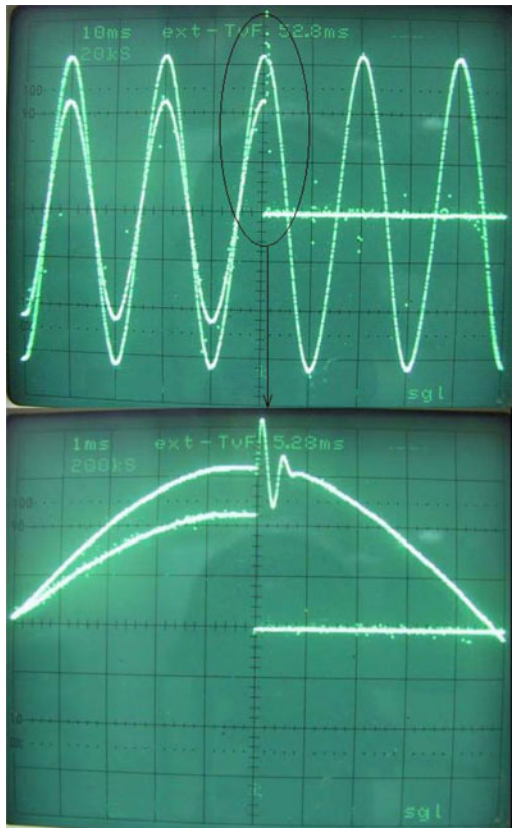

Fig. 16. Experimental result: Transient response of the output voltage for linear step load from 100% to zero, voltage scale = 100 V/div, and current scale = 19 A/div.

TABLE IV
COMPARISON OF INVERTER CHARACTERISTICS: PUBLISHED AND THIS WORK

REF	[6]	[7]	[8]	[10]	[20]	[24]	[25]	This Work
VDC (V)	220V	±100V	120V	300	50	±300	300	360
VAC(Vrms)	140	42	50	110	28	71	210	220
Controller	Deadbeat	Multiple Feedback Loop Control	Virtual Resistor	Multiple Feedback Loop Control	Quasi-Sliding	Multiple Feedback Control	Multiple Feedback Control	Sliding
fsw (kHz)	6.2	2	-	8	20-40	20	5	15
output capacitor (μF)	80	100	200	120	60	-	40	9.4
Inductor (mH)	1.3	5	5	0.2	1.5	-	0.1	0.357
Sout (kVA)	0.6	0.1	0.25	10	0.4	1	1	6
THD(L)	1.20%	2.19%	1.20%	4%	0.30%	1.11%	5%	1.10%
THD(NL)	2.40%	4.07%	4.20%	12%	0.30%	2.70%	-	1.70%
tr* (mSec)	-	-	-	-	2.5	2	-	0.5
OS**	-	-	-	-	-	-	-	29%
US***	-	-	-	-	-12%	-55%	-	-29%

*Transient Time.
**Overshoot in removal step load condition.
***Undershoot in step load condition.

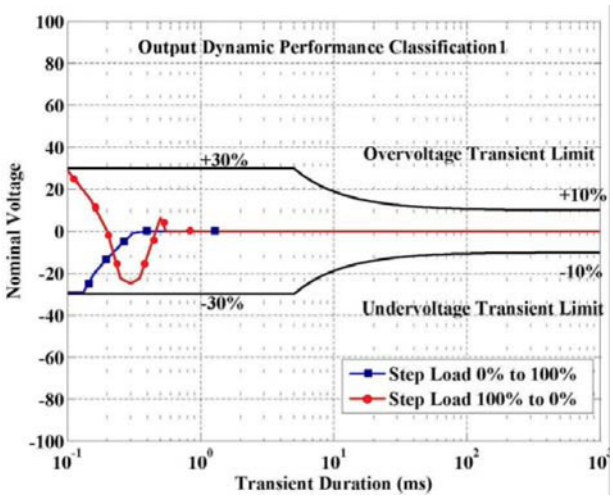

Fig. 17. Output dynamic performance of the inverter.

The experimental waveforms for the dynamic test with linear load are illustrated in Figs. 15 and 16. Fig. 15 shows the linear step loading from 0% to 100% of the rated output active power, and Fig. 16 presents the step load removal from 100% to 0%. The undershoot related to the step load is below 29% and it settles down at 0.3 ms. The overshoot due to the step load removal is also below 29% of rated voltage and it settles down after 0.5 ms. Fig. 17 shows the dynamic deviation of the output voltage at step loading and unloading. It shows that the proposed controller satisfies the voltage limits under dynamic conditions, and it is not exceeding the undervoltage and overvoltage transient limits of classification 1 of the IEC62040-3 standard.

Table IV summarizes the inverter characteristics and compares them with previous works. As can be seen from Table IV, the proposed inverter shows an impressive performance that is better than or comparable to that of the previous works. Although THD of output voltage in [19] is better than this work, its switching frequency is relatively higher and it is variable from 20 to 40 kHz. Moreover, in spite of high switching frequency, it has been used a large output capacitor. Cutoff frequency of the output filter is about 520 Hz in [19], while for this work is about 2800 Hz.

VI. CONCLUSION

In this paper, a fixed frequency SMC was presented for a single-phase inverter. The performance of the proposed controller has been demonstrated by a 6-kVA prototype. Experimental results show that the inverter is categorized in class1 of the IEC64020-3 standard for output dynamic performance. The inverter efficiency was measured up to 95.5% in the worst case.

Since the direct SMC cannot be applied to four switches unipolar inverter and it also suffers from the chattering problem, a PWM is employed to generate a fixed frequency switching law. The PWM modulates the smoothed discontinuous control law which is produced by SMC. To smooth the control law, the limitation of the PWM was considered.

The simulation and experimental results show that the load regulation is about 1% at the steady state as well. But, to obtain better regulation, a resonance compensator was added in the voltage loop. With this compensator, the load regulation was measured which has been below 0.2%.

REFERENCES

[1] G. Venkataramanan and D. M. Divan, "Discrete time integral sliding mode control for discrete pulse modulated converters," in *Proc. 21st Annu. IEEE Power Electron. Spec. Conf.*, San Antonio, TX, 1990, pp. 67–73.

[2] J. Y. Hung, W. Gao, and J. C. Hung, "Variable structure control: A survey," *IEEE Trans. Ind. Electron.*, vol. 40, no. 1, pp. 2–22, Feb. 1993.

[3] E. Fossas and A. Ras, "Second order sliding mode control of a buck converter," in *Proc. 41st IEEE Conf. Decision Control*, 2002, pp. 346–347.

[4] C. Rech, H. Pinheiro, H. A. Gründling, H. L. Hey, and J. R. Pinheiro, "A modified discrete control law for UPS applications," *IEEE Trans. Power Electron.*, vol. 18, no. 5, pp. 1138–1145, Sep. 2003.

[5] K. S. Low, K. L. Zhou, and D. W. Wang, "Digital odd harmonic repetitive control of a single-phase PWM inverter," in *Proc. 30th Annu. Conf. IEEE Ind. Electron. Soc.*, Busan, Korea, Nov. 2–6, 2004, pp. 6–11.

[6] K. Zhang, Y. Kang, J. Xiong, and J. Chen, "Deadbeat control of PWM inverter with repetitive disturbance prediction," in *Proc. 14th Annu. Appl. Power Electron. Conf. Expo.*, 1999, pp. 1026–1031.

[7] N. M. Abdel-Rahim and J. E. Quaicoe, "Analysis and design of a multiple feedback loop control strategy for single-phase voltage- source ups inverters," *IEEE Trans. Power Electron.*, vol. 11, no. 4, pp. 532–541, Jul. 1996.

[8] P. A. Dahono and E. Taryana, "A new control method for single-phase PWM inverters to realize zero steady-state error and fast response," in *Proc. 15th Int. Conf. Power Electron. Drive Syst.*, 2003, pp. 888–892.

[9] J. Wang, L. Liu, F. Zhang, C. Gong, and Y. Ma, "Modeling and analysis of hysteretic current mode control inverter," in *Proc. 24th Annu. IEEE Appl. Power Electron. Conf. Expo.*, 2009, pp. 1338–1343.

[10] Y. T. Woo and Y. C. Kim, "A digital control of a single-phase ups inverter for robust ac-voltage tracking," in *Proc. 30th Annu. Conf. IEEE Ind. Electron. Soc.*, Busan, Korea, Nov. 2–6, 2004, pp. 1623–1628.

[11] P. Cortés, G. Ortiz, J. I. Yuz, J. Rodríguez, S. Vazquez, and L. G. Franquelo, "Model predictive control of an inverter with output LC filter for UPS applications," *IEEE Trans. Ind. Electron.*, vol. 56, no. 6, pp. 1875–1883, Jun. 2009.

[12] G. Venkataramanan and D. M. Divan, "Discrete time integral sliding mode control for discrete pulse modulated converters," in *Proc. 21st Annu. IEEE Power Electron. Spec. Conf.*, 1990, pp. 67–73.

[13] H. Erdem, "Comparison of fuzzy, PI and fixed frequency sliding mode controller for DC–DC converters," in *Proc. Int. Aegean Conf. Elect. Mach. Power Electron.*, 2007, pp. 684–689.

[14] M. Ahmed, M. Kuisma, K. Tolsa, and P. Silventoinen, "Standard procedure for modeling the basic three converters (buck, boost, and buck-boost) with PID algorithm applied," in *Proc. 13th Int. Symp. Electr. Apparatus Technol., SIELA 2003*, Plovdive, Bulgaria, May 29–30, 2003.

[15] J. Hu, L. Shang, Y. He, and Z. Q. Zhu, "Direct active and reactive power regulation of grid-connected DC/AC converters using sliding mode control approach," *IEEE Trans. Power Electron.*, vol. 26, no. 1, pp. 210–222, Jan. 2011.

[16] K. D. Young and U. Ozguner, "Sliding mode: Control engineering in practice," in *Proc. Amer. Control Conf.*, San Diego, CA, Jun. 1999, pp. 150–162.

[17] S.-C. Tan, Y. M. Lai, C. K. Tse, and M. K. H. Cheung, "Adaptive feedforward and feedback control schemes for sliding mode controlled power converters," *IEEE Trans. Power Electron.*, vol. 21, no. 1, pp. 182–192, Jan. 2006.

[18] S.-C. Tan, Y. M. Lai, C. K. Tse, and M. K. H. Cheung, "A fixed-frequency pulsewidth modulation based quasi-sliding-mode controller for buck converters," *IEEE Trans. Power Electron.*, vol. 20, no. 6, pp. 1379–1392, Nov. 2005.

[19] R. R. Ramos, D. Biel, E. Fossas, and F. Guinjoan, "A fixed-frequency quasi-sliding control algorithm: Application to power inverters design by means of FPGA implementation," *IEEE Trans. Power Electron.*, vol. 18, no. 1, pp. 344–355, Jan. 2003.

[20] A. A. Ahmad, A. Abrishamifar, and S. Elahian, "Fixed frequency sliding mode controller for the buck converter," in *Proc. 2nd Power Electron., Drive Syst. Technol. Conf.*, Tehran, Iran, Feb. 2011, pp. 557–561.

[21] Ahmad, A. Ale, A. Abrishamifar, and M. Farzi, "A new design procedure for output LC filter of single phase inverters," presented at the 3rd Int. Conf. Power Electron. Intell. Transp. Syst., Shenzhen, China, Nov. 2010.

[22] J.-J. E. Slotine and W. Li, *Applied Nonlinear Control*. Englewood Cliffs, NJ: Prentice-Hall, 1991.

[23] D. G. Holmes, T. A. Lipo, B. P. McGrath, and W. Y. Kong, "Optimized design of stationary frame three phase ac current regulators," *IEEE Trans. Power Electron.*, vol. 24, no. 11, pp. 2417–2426, Nov. 2009.

[24] W. Guo, S. Duan, Y. Kang, and J. Chen, "A new digital multiple feedback control strategy for single-phase voltage-source PWM inverters," in *Proc. Int. Conf. Elect. Electron. Technol.*, Aug. 2001, vol. 2, pp. 809–813.

[25] A. M. Salamah, S. J. Finney, and B. W. Williams, "Single-phase voltage source inverter with a bidirectional buck–boost stage for harmonic injection and distributed generation," *IEEE Trans. Power Electron.*, vol. 24, no. 2, pp. 376–387, Feb. 2009.

Adib Abrishamifar (M'08) was born in Tehran, Iran, in 1967. He received the B.S., M.S., and Ph.D. degrees in electronics engineering from the Iran University of Science and Technology (IUST), Tehran, Iran, in 1989, 1992, and 2001, respectively.

Since 1993, he has been with the Department of Electrical Engineering, IUST. His current research interests include analog integrated circuit design and power electronics.

Ahmad Ale Ahmad was born in Babol, Iran, on August 6, 1980. He received the B.S. and M.S. degrees in electrical engineering from the Iran University of Science and Technology (IUST), Tehran, Iran, in 2002 and 2006, respectively. Currently, he is a Ph.D. student at IUST.

Since 2002, he has been with the Iranian Research Institute of Electrical Engineering, Tehran, Iran, designing medium and high power converter. His current research interests include high-voltage voltage source converter.

Mustafa Mohamadian (M'06) received the B.S. degree in electrical engineering from the AmirKabir University of Technology, Tehran, Iran, in 1989, the M.S. degree in electrical engineering from Tehran University, Tehran, Iran, in 1992, and the Ph.D. degree in electrical engineering, specializing in power electronics, from the University of Calgary, Calgary, AB, Canada, in 1997.

He is currently an Associate Professor in the Department of Electrical and Computer Engineering, Tarbiat Modares University, Tehran, Iran. His research interests include analysis, modeling, and control of power converters, renewable energy systems, uninterruptible power supplies, and motor drives, and real-time embedded software development for power electronics applications using microcontrollers and DSPs.